

Bubbly Cavitating Flow Through a Converging Nozzle

Mohammed ZAMOUM¹, Rachid BOUCETTA¹, Mohand KASSEL¹

Laboratoire Génie Physique des Hydrocarbures LGPH, Faculté des Hydrocarbures et de la Chimie FHC,
Université M'hamed Bougara Boumerdes UMBB
Boulevard de l'indépendance, Boumerdes 35000, Algeria
m.zamoum@univ-boumerdes.dz; r.boucetta@univ-boumerdes.dz
m.kessal@univ-boumerdes.dz

Abstract- In the present work, the bubbly cavitating flow phenomena after passing through the converging nozzle is numerically investigated. The dynamic of the cavitating bubbles is modeled by the use of the mass and momentum phase's equations, which are coupled with the Rayleigh-Plesset equation of the N bubbles dynamics. However, assuming that the same initial conditions of all bubbles are identical and that all bubbles are equi-distant from each other simplifies the governing equations. Equation set is numerically resolved by the use of a fourth order Runge-Kutta scheme. The numerical resolution of the previous equations set let us found that the bubble radius distribution, fluid velocity and fluid pressure change dramatically with upstream void fraction and an instability appeared just after the passing the converging nozzle for both cases one bubble N=1 and two bubbles N=2. Indeed, for the case of one bubble N=1, the flashing flow phenomena occurs for an upstream void fraction $\alpha_s=11.2 \times 10^{-3}$, which corresponds to a critical bubble radius $R_c=1.8$. Whereas, for bubble number N=2, the same phenomenon occurs for $\alpha_s = 8.9 \times 10^{-3}$, with $R_c=2$. This difference is due to the bubble interaction. Also, we found that, the bubble number N strongly affect the bubble frequency. However, with increase the bubble number, the maximum size of the bubbles increases and bubble frequency oscillation decrease.

Keywords: Bubbly flow, Converging nozzle, Two phase flow, Cavitation

1. Introduction

Bubbly cavitating flows in ducts and nozzles represent an important problem in many engineering applications such as propelling nozzles in jet engines. The converging nozzle flow is one of any cavitating flow in which a low pressure region causes the flow to accelerate. The investigations of homogeneous steady-state cavitating nozzle flows, using spherical bubble dynamics with a polytropic thermal process [1, 2], have shown some flow instabilities illustrated by flashing flow phenomenon.

The flow model, a generally used, is a nonlinear continuum bubbly mixture which is coupled with the dynamics equation of the bubble. A three equations model was first proposed by van Wijngaarden [3, 4] and has been used for studying steady and transient shock wave propagation in bubbly liquids, by omitting the acceleration of the mean flow. This model has been also considered by Wang and Brennen [1], in the case of converging-diverging nozzle, with an upstream variable void fraction. It was observed that significant change of the flow characteristics depends strongly on the latter and a critical bubbles radius have been obtained.

A. Ooi and R. Manasseh [5] have studied coupling effects on acoustic signature from non-linear oscillations of a group of micro bubbles by the use of Rayleigh-Plesset equation, where bubbles number and their natural frequency are significantly dependant.

Several numerical and experimental studies have been carried out on the effect of the geometrical parameters [6, 9], such as throat diameter, throat length, and diffuser angle, on the mass flow rate, critical pressure ratio and application rang of small-sized cavitating venturi. Also, Tian et al [10] have designed and investigated a variable area cavitating venture. They have realised four sets of experiments to investigate the effect of the pintle stroke, the upstream pressure and downstream pressure as well as the dynamic motion of the pintle on the performance of the variable area cavitating venture. They concluded that the variable area cavitating venturi can control and measure the mass flow rate dynamically.

More recently, Zamoum et al [11] have numerically investigated the dynamical of a bubbly flows converging-diverging nozzle (Venturi). The mass and momentum phases equations, which are coupled with the Rayleigh-Plesset

equation of the bubbles dynamics are used. The effects of upstream void fraction, bubbles number and distance between bubbles are investigated. The numerical resolution of the equations set (ODE) found that the bubble radius change dramatically with upstream void fraction and an instability appeared just after the throat of the Venturi for both cases one bubble (N=1) and two bubbles (N=2).

The present work considers new model of bubbly cavitating flow. This model is composed by mass and momentum equation coupled with the dynamic equation of N bubbles. Equation set is numerically resolved by the use of a fourth order Runge-Kutta scheme. The effects of upstream void fraction and bubbles number on the bubble radius distribution, fluid velocity and fluid pressure after passing the converging nozzle are investigated.

2. Theory and Basic Equations

The liquid is assumed to be incompressible and the interaction liquid duct wall is neglected. The total upstream bubbles population is uniform without coalescence, and the relative motion between the phases ignored. Gas and vapour densities are neglected in comparison to one of the liquid. The bubbles are assumed to have the same initial radius R_s and external friction is neglected.

The dynamics of the bubbles can be modelled by the Rayleigh-Plesset equation [5]

$$\rho_L^* \left[R^* \frac{d^2 R}{dt^{*2}} + \frac{3}{2} \left(\frac{dR^*}{dt^*} \right)^2 \right] + \frac{4\mu_E^*}{R^*} \frac{dR^*}{dt^*} = \left(p_s^* - p_v^* + \frac{2S^*}{R_s^*} \right) \left(\frac{R_s^*}{R^*} \right)^{3k} - p^* + p_v^* - \frac{2S^*}{R^*} - p_{ext}^* \quad (1)$$

Where $R^*(t)$ is the instantaneous bubble radius, R_s^* the upstream bubble radius, μ_E^* the effective dynamic viscosity of the liquid, ρ_L^* the density of the liquid, p_s^* the upstream pressure, p_v^* the vapor pressure, S^* the surface tension of the liquid, p^* the fluid pressure and p_{ext}^* is the imposed external pressure field, where:

$$p_{ext}^* = p_{si}^* + p_{A,i}(t) \quad (2)$$

Where

$$p_{si}^* = \sum_{j \neq i}^{Nbub} \frac{\rho_L^*}{s_{ij}} \frac{d}{dt^*} \left(R_j^{*2} \frac{dR_j^*}{dt^*} \right) \text{ is the pressure scattered by the other bubbles.}$$

Where $s_{ij}=s_{ji}$ is the distance of bubble i from bubble j , $p_{A,i}(t)$ the applied pressure of any external field on bubble i . Combining equations (1) and (2) gives the following coupled governing equation for coupled bubble oscillations,

$$\rho_L^* \left[R^* \frac{d^2 R}{dt^{*2}} + \frac{3}{2} \left(\frac{dR^*}{dt^*} \right)^2 \right] + \frac{4\mu_E^*}{R^*} \frac{dR^*}{dt^*} = \left(p_s^* - p_v^* + \frac{2S^*}{R_s^*} \right) \left(\frac{R_s^*}{R^*} \right)^{3k} - p^* + p_v^* - \frac{2S^*}{R^*} - \sum_{j \neq i}^{Nbub} \frac{\rho_L^*}{s_{ij}} \frac{d}{dt^*} \left(R_j^{*2} \frac{dR_j^*}{dt^*} \right) - P_{A,i}(t^*) \quad (3)$$

We assume that $s_{ij}=D$ = constant. Thus the distance of any bubble to any other bubble in the bubble population is constant. We further assume that the same external driving pressure field acts on all the bubbles, that is, $P_{A,1}(t^*)=P_{A,2}(t^*)=P_{A,3}(t^*)=P_{A,4}(t^*)=P_A(t^*)$, then $R_i^*(t^*)=R_j^*(t^*)=R^*(t^*)$.

Substituting into equation (3) yields:

$$\rho_L^* \left[R^* \frac{d^2 R^*}{dt^{*2}} + \frac{3}{2} \left(\frac{dR^*}{dt^*} \right)^2 \right] + \frac{4\mu_E^*}{R^*} \frac{dR^*}{dt^*} = \left(p_s^* - p_v^* + \frac{2S^*}{R_s^*} \right) \left(\frac{R_s^*}{R^*} \right)^{3k} - p^* + p_v^* - \frac{2S^*}{R^*} - (N_{bub} - 1) \frac{\rho_L^*}{D} \left(R^{*2} \frac{d^2 R^*}{dt^{*2}} \right) - (N_{bub} - 1) \frac{2\rho_L^*}{D} \left(R^* \left(\frac{dR^*}{dt^*} \right)^2 \right) - P_A^*(t^*) \quad (4)$$

Equation (4) represents the idealized case where all the bubbles are equally spaced, have the same initial conditions. The non-dimensional form equation (4) is giving by:

$$R \frac{D^2 R}{Dt^2} + \frac{3}{2} \left(\frac{DR}{Dt} \right)^2 + \frac{\sigma}{2} (1 - R^{-3k}) + \frac{4}{Re} \frac{1}{R} \frac{DR}{Dt} + \frac{2}{We} (R^{-1} - R^{-3k}) + \frac{1}{2} Cp + (N_{bub} - 1) \frac{R_s^{*2} u_s^{*2}}{D} R^2 \frac{D^2 R}{Dt^2} + (N_{bub} - 1) \frac{2R_s^* u_s^{*2}}{D} R \left(\frac{DR}{Dt} \right)^2 + P_A = 0 \quad (5)$$

Where $D/Dt = \partial/\partial t + u\partial/\partial x$ is the Lagrangian derivative, $\sigma = (p_s^* - p_v^*)/1/2\rho_L^* u_s^{*2}$ is the cavitation number, p_v^* is the partial pressure of vapor inside the bubble. $Re = \rho_L^* u_s^* R_s^*/\mu_E^*$ is the Reynolds number, μ_E^* is the effective viscosity of liquid. $We = \rho_L^* u_s^{*2} R_s^*/S^*$ is the Weber number, S^* is the liquid surface tension and ρ_L^* is the liquid density.

Continuity and momentum equations of the bubbly flow (Wang and Brennen 1998) [1] are:

$$\frac{\partial}{\partial t} [(1-\alpha)A] + \frac{\partial}{\partial x} [(1-\alpha)uA] = 0 \quad (6)$$

$$\frac{\partial u}{\partial t} + u \frac{\partial u}{\partial x} = -\frac{1}{2(1-\alpha)} \frac{\partial Cp}{\partial x} \quad (7)$$

Where $\alpha(x, t) = 4/3\pi\eta R^3 / [1 + 4/3\pi\eta R^3]$ is the bubble void fraction, $u(x, t)$ the fluid velocity. $Cp(x, t) = (p^*(x, t) - p_s^*)/1/2\rho_L^* u_s^{*2}$ the fluid pressure coefficient, $p(x, t)$ the fluid pressure, p_s^* the upstream fluid pressure, and u_s^* is the upstream fluid velocity.

Equations (5), (6) and (7) constitutes a simple model of one-dimensional flowing bubbles fluid with nonlinear bubbles dynamics.

Assuming steady-state conditions, all the partial time derivative terms in equations (5),(6) and (7) disappear. Then, the former equation set is transformed into an ordinary differential equation set, with only one independent variable (x):

$$(1-\alpha)uA = (1-\alpha_s) = constant \quad (8)$$

$$u \frac{du}{dx} = -\frac{1}{2(1-\alpha)} \frac{dCp}{dx} \quad (9)$$

$$R \left(u^2 \frac{d^2 R}{dx^2} + u \frac{du}{dx} \frac{dR}{dx} \right) \times \left(1 + \frac{(N-1)}{D} R_s u_s^2 R \right) + \frac{3u^2}{2} \left(\frac{dR}{dx} \right)^2 + 2 \frac{(N-1)}{D} R_s u_s^2 R u^2 \left(\frac{dR}{dx} \right)^2 + \frac{4}{Re} \frac{u}{R} \frac{dR}{dx} + \frac{2}{We} \left(\frac{1}{R} - \frac{1}{R^{3k}} \right) + \frac{\sigma}{2} \left(1 - \frac{1}{R^{3k}} \right) + \frac{1}{2} Cp = 0 \quad (10)$$

The corresponding initial conditions are:

$$R(x=0)=1, U(x=0)=1, Cp(x=0)=0$$

And the axial variation of the cross sectional takes the following from:

$$A(x) = \begin{cases} 1 & 0 < x < x_1 \\ 1 - \frac{(x-x_1)(1-\beta)}{x_2-x_1} & x_1 < x < x_2 \\ \beta & x_2 < x < x_3 \end{cases} \quad (11)$$

Where β is the dimensionless radius of the diverging throat and x the distance along the axis. In the present work it is assumed: $\beta=0.8$, $x_1=3$, $x_2=5.7$

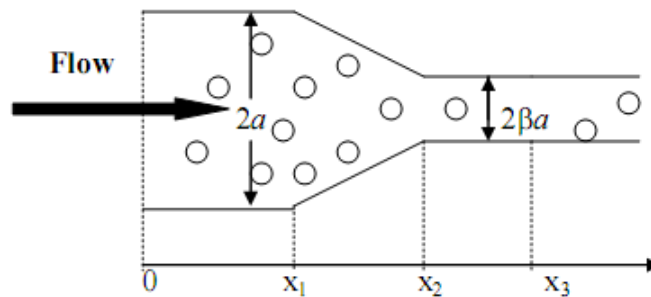


Fig. 1: Bubbly flow through a converging nozzle.

3. Results and Discussion

Equation set (8)-(9) and (10) is resolved by the use of a fourth order Runge-Kutta scheme, with some flow conditions (Table 1).

Table 1: Initials conditions flow and water characteristics.

Initial parameters	Water characteristics at 20°C
$R_s^* = 100\mu\text{m}$	$\rho_L^* = 1000\text{kg/m}^3$
$u_s^* = 10\text{m/s}$	$\mu_E^* = 0.03\text{Ns/m}^2$
$k=1.4$	$\mu_L^* = 0.001\text{Ns/m}^2$
$Re=33$	$S^* = 0.073\text{N/m}$
$\sigma=0.8$	
$We=137$	

3.1. Upstream Void Fraction Effect for One Bubble (N=1)

Six different upstream void fractions (α_s) of the order of 10^{-3} are used in the computation to study, the effect of the upstream void fraction on the flow structure through a converging nozzle. The case of $\alpha_s=0$ corresponds to the incompressible pure liquid flow, the results are shown in Figures 2 and 3 which correspond to the non-dimensional bubble radius distribution, fluid velocity and fluid pressure coefficient, respectively, an instability inception can be remarked in these figures, which is located just after passing converging section, these results confirm those of Wang and Brennen [1] and Zamoum et al [2] for converging diverging nozzle and Venturi nozzle respectively.

Figure 2 shown that the bubble size reach the maximum after passing the converging nozzle and with increase in the upstream void fraction, the maximum size of the bubbles increases and bubble frequency oscillation decrease, this maximum size is shifted further downstream after it reach the critical radius (instability occurs), the bubbles growth without bound in the calculation, this instability occurs when the bubble reaches a critical value, also the void fraction growing leads to large amplitudes of the previously down parameters. It can be observed that instability occurs for an upstream void fraction $\alpha_s=1.12 \times 10^{-2}$, which corresponds to a critical bubble radius $R_c = 1.8$. In the practice R_c correspond the flashing flow inception.

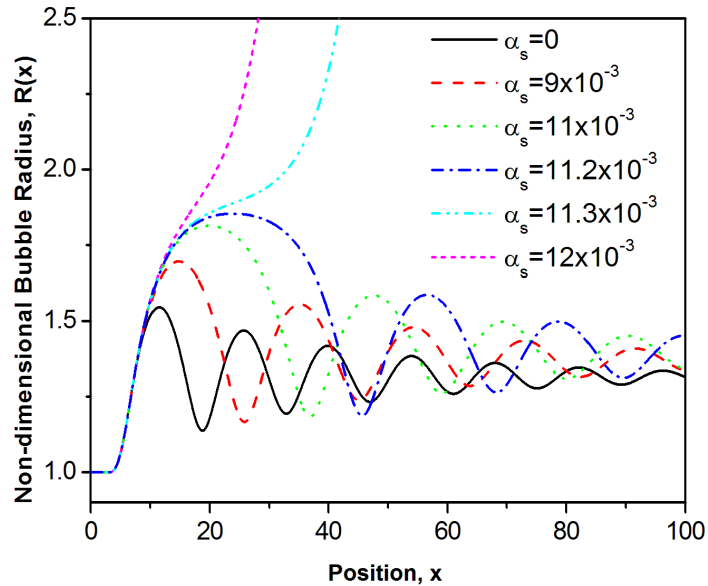


Fig. 2: Non-dimensional bubble radius distribution as a function of the position in the flow for different upstream void fraction and for the case of one bubble N=1.

The fluid velocity and the fluid pressure coefficient are illustrated in Figure 3. The presence of the bubble in the upstream flow results in the downstream fluctuations of the flow. With increase the upstream void fraction, the amplitude of this velocity fluctuations downstream increase and its frequency oscillation decrease. However, as α_s increases to a critical value of the upstream void fraction, the flashing flow occurs, the velocity increases dramatically and the flow becomes unstable. Due to the Bernoulli effects, the fluid pressure coefficient varies inversely with the fluid velocity (Figure 3).

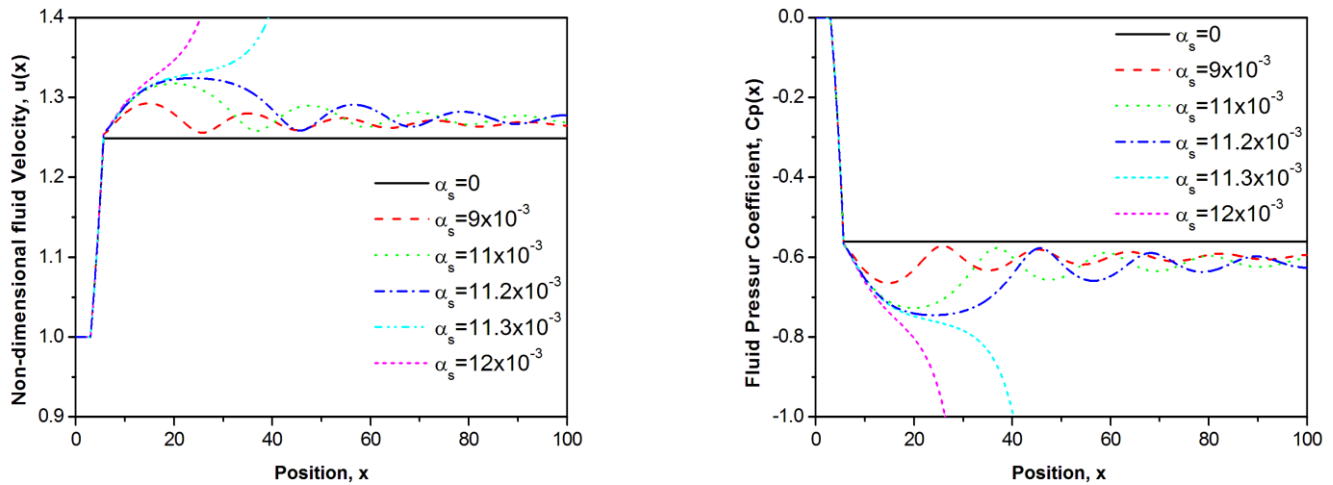


Fig. 3: Non-dimensional fluid velocity distribution $u(x)$ and fluid pressure coefficient $C_p(x)$ as a function of the position in the flow for different upstream void fraction and for the case of one bubble $N=1$.

3.1. Upstream Void Fraction Effect for two Bubbles ($N=2$)

Five different upstream void fractions (α_s) are used in the computation to study the effect of the upstream void fraction on the flow structure through the converging nozzle. The results are shown in Figures 4 and 5 which correspond to the non-dimensional bubble radius, fluid velocity and fluid pressure distributions for case of two bubbles ($N=2$). An instability inception can be remarked in these figures, which is located just after the converging section. It can be observed that, for the case of two bubbles, the instability occurs for an upstream void fraction $\alpha_s=8.9 \times 10^{-3}$, which corresponds to a critical bubble radius $R_c=2$ (Figure 4). Whereas, for bubble number $N=1$, the same phenomenon occurs for $\alpha_s = 1.12 \times 10^{-2}$, with $R_c=1.8$. This difference is due to the bubble interaction. Also, it can be observed that, the bubble number N strongly affect the bubble frequency. With increase the bubble number, the maximum size of the bubbles increases and bubble frequency oscillation decrease. The latter is also observed in Figure 5 for the fluid velocity $u(x)$ and pressure $C_p(x)$ distributions

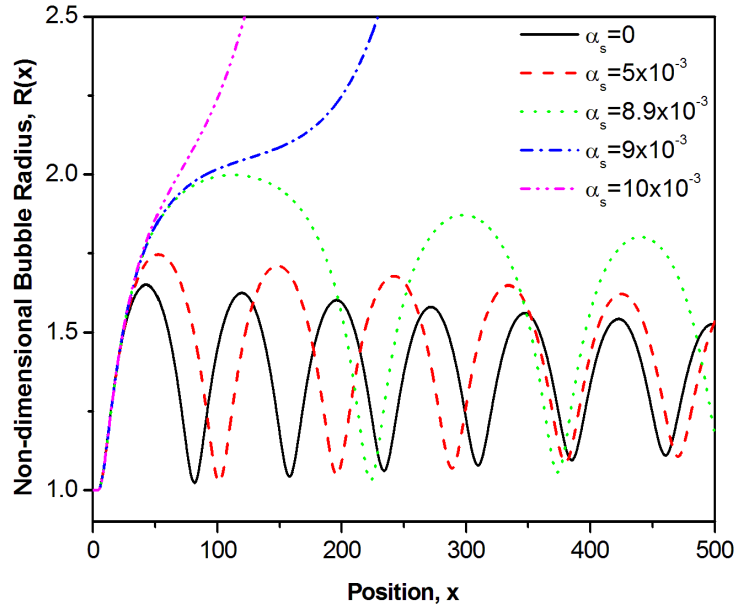


Fig. 4: Non-dimensional bubble radius distribution as a function of the position in the flow for different upstream void fraction and for the case of two bubbles, $N=2$.

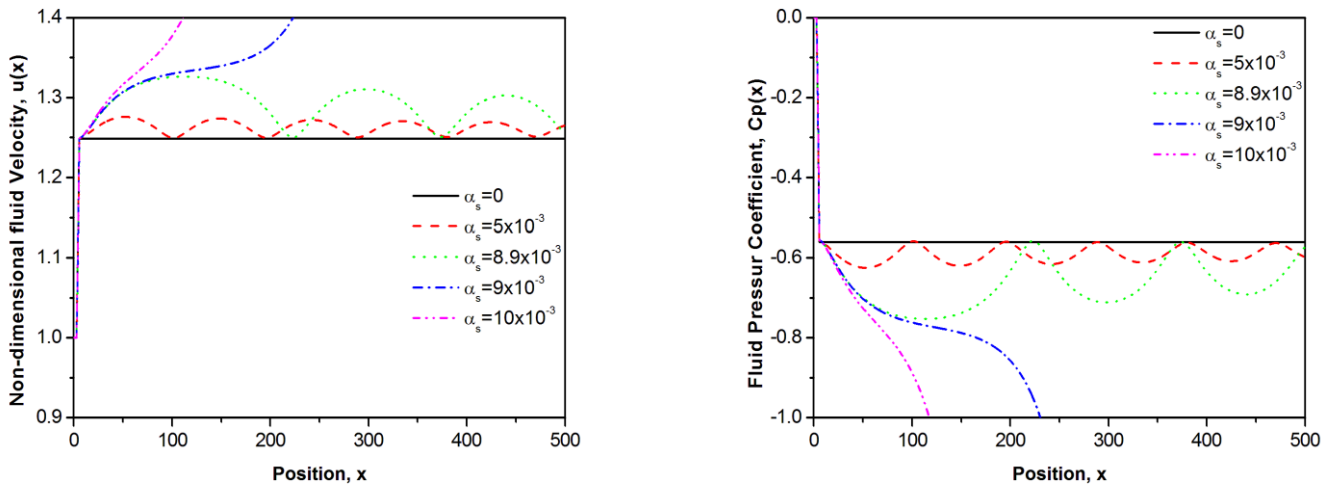


Fig. 5: Non-dimensional fluid velocity distribution $u(x)$ and fluid pressure coefficient $C_p(x)$ as a function of the position in the flow for different upstream void fraction and for the case of two bubbles, $N=2$.

4. Conclusion

The dynamic of the cavitating bubbles through a converging nozzle is modeled by the use of the mass and momentum phase's equations, which are coupled with the Rayleigh-Plesset equation of the N bubbles dynamics. Equation set is numerically resolved by the use of a fourth order Runge-Kutta scheme. We have shown the effects of upstream void fraction and bubbles number on the bubble radius distribution, fluid velocity and fluid pressure after passing the converging nozzle. In the obtained result, we found that the upstream void fraction strongly affect the structure of the flow. Two different flow regimes are obtained: quasi-steady and quasi-unsteady regimes, where the transition between them is illustrated by a flashing flow inception. In the case of one bubble $N=1$, the flashing flow phenomena occurs for an upstream void fraction $\alpha_s=11.2 \times 10^{-3}$, which corresponds to a critical bubble radius $R_c=1.8$. Whereas, for bubble number $N=2$, the same phenomenon occurs for $\alpha_s = 8.9 \times 10^{-3}$, with $R_c=2$. This difference is due to the bubble interaction. Also, we found that, the bubble number N strongly affect the bubble frequency. With increase the bubble number, the maximum size of the bubbles increases and bubble frequency oscillation decrease.

5. Nomenclature

A	dimensionless cross-sectional area	Greek Letters	
D	distance between bubbles		
k	polytropic index for the gas inside the bubbles	α	void fraction of the bubbly fluid
R	dimensionless bubble radius, R^*/R_s^*	β	dimensionless radius of the converging nozzle
S*	surface tension of the liquid	η	dimensionless bubble population per unit liquid volume, $\eta^*R_s^{*3}$
t	dimensionless time, $t^*u_s^*/R_s^*$	γ	ratio of specific heats of the gas inside the bubbles
u	dimensionless fluid velocity, u^*/u_s^*	μ_E^*	effective dynamic viscosity of the liquid
V	volume of the bubble, $V = 4/3\pi R^3$	ρ	dimensionless fluid density
x	dimensionless Eulerian coordinate, x^*/R_s^*	ρ_L^*	density of the liquid

References

- [1] Wang, Y.-C and Brennen, C. E. One-Dimensional Bubbly Cavitating Flows Through a Converging-Diverging Nozzle. *Journal of Fluids Engineering*, 120, pp. 166-170, 1998
- [2] Zamoum. M and Kessal. M. Analysis of cavitating flow through a Venturi. *Scientific Research and Essays*. Vol 10 (11) pp 367-375, 2015.
- [3] van Wijngaarden, L. One the equations of motion for mixtures of liquid and gas bubbles. *Journal of fluid mechanics*, vol. 33, pp. 465-474, 1968
- [4] van Wijngaarden, L. One-dimensional flow of liquids containing small gas bubbles. *Annual review of fluid mechanics*, 4, pp. 369-396, 1972
- [5] Ooi. A and Manasseh. R. Coupled nonlinear oscillations of microbubbles. *AZIAM*. J. 46(E). pp C102_C116, 2005
- [6] Wang, Y.-C and Brennen, C. E. Numerical computation of shock waves in a spherical bubble cloud of cavitation bubbles. *Journal of Fluids Engineering*, 121, 872-880,1999
- [7] Soubiran, J. and Sherwood, J. D. Bubble motion in a potential flow within a Venturi . *journal of multiphase flow*, vol. 26, pp. 1771-1796, 2000
- [8] Moholkar, V. S., and Pandit, A.B. Numerical investigations in the behaviour of one-dimensional bubbly flow in hydrodynamic cavitation. *Chemical Engineering Science*, vol. 56, pp. 1411-1418, 2001
- [9] Ashrafizadeh SM, Ghassemi H . Experimental and numerical investigation on the performance of small-sized cavitating venturi. *Flow measurement and Instrumentation*, 42: pp. 6-15, 2015
- [10] Tian H, Zeng P, Yu N, Cai G. Application of variable area cavitating venturi as a dynamic flow controller. 38: 21-26, 2014
- [11] M. Zamoum, R. Boucetta, M. Kessal. Modeling and Numerical Investigations in the Behavior of One-dimensional bubbly Cavitating Flows Through a Venturi. *24^{ème} Congrès de Mécanique Brest*, 26 au 30 Aout 2019.